Springer

Journal of Mechanical Science and Technology 23 (2009) 291~301

Journal of Mechanical Science and Technology

www.springerlink.com/content/1738-494x
DOI 10.1007/s12206-008-1110-5

Hilbert-Huang transform and marginal spectrum for detection and diagnosis of localized defects in roller bearings †

Hui Li[1,*], Yuping Zhang[1] and Haiqi Zheng[2]

[1]*Department of Electromechanical Engineering, Shijiazhuang Institute of Railway Technology, Shijiazhuang, 050041, P.R. China*
[2]*First Department, Shijiazhuang Mechanical Engineering College, Shijiazhuang, 050003, P.R. China*

(Manuscript Received November 27, 2007; Revised September 3, 2008; Accepted November 12, 2008)

Abstract

This work presents the application of a new signal processing technique, the Hilbert-Huang transform and its marginal spectrum, in analysis of vibration signals and fault diagnosis of roller bearings. The empirical mode decomposition (EMD), Hilbert-Huang transform (HHT) and marginal spectrum are introduced. First, the vibration signals are separated into several intrinsic mode functions (IMFs) by using EMD. Then the marginal spectrum of each IMF can be obtained. According to the marginal spectrum, the localized fault in a roller bearing can be detected and fault patterns can be identified. The experimental results show that the proposed method may provide not only an increase in the spectral resolution but also reliability for the fault detection and diagnosis of roller bearings.

Keywords: Bearing; Faults diagnosis; Empirical mode decomposition; Hilbert-Huang transform; Signal processing; Marginal spectrum

1. Introduction

Bearings are an important element in a variety of industrial applications such as machine tool and gearbox. An unexpected failure of the bearing may cause significant economic losses. For that reason, fault detection and diagnosis of bearings has been the subject of intensive research. Vibration signal analysis has been widely used in the faults detection of rotation machinery. Many methods based on vibration signal analysis have been developed. These methods include power spectrum estimation, fast Fourier transform (FFT), envelope spectrum analysis, which have proven to be effective in bearing fault detection. However, these methods are based on the assumption of stationarity and linearity of the vibration signal. Therefore, new techniques are needed to analyze vibration for fault detection in roller bearings. Bearing faults by their nature are time localized transient events. To deal with non-stationary and non-linear signals, time-frequency analysis techniques such as the short time Fourier transform (STFT) [1], wavelet transform (WT) [2-6] and Wigner-Ville distribution (WVD) [7-11] are widely used. The STFT [1] uses sliding windows in time to capture the frequency characteristics as functions of time. Therefore, a spectrum is generated at discrete time instants. An inherent drawback with the STFT is the limitation between time and frequency resolutions. A finer frequency resolution can only be achieved at the expense of time resolution and vice-versa. Furthermore, this method requires large amounts of computation and storage for display. The wavelet transform (WT), on the other hand, is similar to the STFT in that it also provides a time-frequency map of the signal being analyzed. The improvement that the WT makes over the STFT is that it can achieve high frequency resolution with sharper time resolutions. A very appealing feature of the wavelet analysis is that it provides a uniform resolution for all the scales. Limited by the size of the basic wavelet

† This paper was recommended for publication in revised form by Associate Editor Seong-Wook Hong

* Corresponding author. Tel.: +86 311 8862 1089, Fax.: +86 311 8862 1073
E-mail address: Huili68@163.com

© KSME & Springer 2009

function, the downside of the uniform resolution is uniformly poor resolution. Moreover, an important limitation of the wavelet analysis is its non-adaptive nature. Once the basic wavelet is selected, one has to use it to analyze all the data. This leads to a subjective assumption on the characteristic of the analyzed signal. As a consequence, only signal features that correlate well with the shape of the wavelet function have a chance to lead to coefficients of high value. All other feature will be masked or completely ignored. The WVD is a basic time-frequency representation, which is part of the Cohen class of distribution. Furthermore, it possesses a great number of good properties and is of popular interest for non-stationary signal analysis. Therefore, the Wigner-Ville distribution has received considerable attention in recent years as an analysis tool for non-stationary or time-varying signals. It has been widely used in the areas of structure-bone noise identification [12], optics [13], and machinery condition monitoring [14-16] and so on. The difficulty with this method is the severe cross terms as indicated by the existence of negative power for some frequency ranges. In addition, the WVD of discrete time signals suffers from the aliasing problem, which may be overcome by employing various approaches.

In this work, we introduce a novel approach for nonlinear, non-stationary data analysis. An application of the Hilbert-Huang transform method to fault diagnosis of bearings is presented. The methodology developed in this paper decomposes the original times series data in intrinsic oscillation modes, using the empirical mode decomposition. Then, the Hilbert transform is applied to each intrinsic mode function, therefore, the time-frequency distribution is obtained. The basic method is introduced in detail. The Hilbert-Huang transform is applied in the research of the fault diagnosis of bearing faults. The experimental results show that this method can effectively detect and diagnose the roller bearing faults.

This paper is organized as follows: Section 1 gives a brief introduction of the time-frequency analysis technology. Section 2 gives a brief description of the Hilbert-Huang transformation (HHT). Section 3 presents the method and procedure of the fault diagnosis based on HHT and marginal spectrum. Section 4 gives a simulation example to provide the comparisons among the FFT, Morlet wavelet spectrum, STFT spectrum and Hilbert-Huang transform spectrum in order to show the novelty and reliability of the proposed method. Section 5 describes the experimental set-up. Section 6 gives the applications of the method based on marginal spectrum to faults detection and diagnosis of roller bearing. Section 7 gives the main conclusions of this paper.

2. An introduction to the Hilbert-Huang Transform [17]

Hilbert-Huang transformation is an emerging novel technique of signal decomposition having many interesting properties. In particular, HHT has been applied to numerous scientific investigations, such as biomedical signals processing [18-20], geophysics [21-24], image processing [25], structural testing [26], fault diagnosis [27-29], nuclear physics [30] and so on. In order to facilitate the reading of this paper we will introduce in detail the Hilbert-Huang transformation, which is a relatively novel technique.

2.1 The concept of intrinsic mode function (IMF)

Physically, the necessary conditions for us to define a meaningful instantaneous frequency are that the functions are symmetric with respect to the local zero mean, and have the same numbers of zero crossings and extrema. Based on these observations, Huang et al. [17] defined IMF as a class of functions that satisfy two conditions:

1) In the whole data set, the number of extrema and the number of zero-crossings must be either equal or differ at most by one.

2) At any point, the mean value of the envelope defined by the local maxima and the envelope defined by the local minima is zero.

The first condition is obvious; it is similar to the traditional narrow band requirements for a stationary Gaussian process. The second condition is a new idea; it modifies the classical global requirement to a local one; it is necessary so that the instantaneous frequency will not have unwanted fluctuations induced by asymmetric wave forms. Ideally, the requirement should be 'the local mean of the data being zero'. For non-stationary data, the 'local mean' involves a 'local time scale' to compute the mean, which is impossible to define. As a surrogate, we use the local mean of the envelopes defined by the local maxima and the local minima to force the local symmetry instead. This is a necessary approximation to avoid the definition of a local averaging time scale. Although it will introduce an alias in the instantaneous frequency for nonlinearly deformed waves, the

effects of non-linearity are much weaker in comparison with the non-stationary, as we will discuss later. With the physical approach and the approximation adopted here, the method does not always guarantee a perfect instantaneous frequency under all conditions. Nevertheless, we will show that, even under the worst conditions, the instantaneous frequency so defined is still consistent with the physics of the system studied.

The name 'intrinsic mode function' is adopted because it represents the oscillation mode imbedded in the data. With this definition, the IMF in each cycle, defined by the zero crossings, involves only one mode of oscillation; no complex riding waves are allowed. With this definition, an IMF is not restricted to a narrow band signal, and it can be both amplitude and frequency modulated. In fact, it can be non-stationary. As discussed above, purely frequency or amplitude modulated functions can be IMFs even though they have a finite bandwidth as defined traditionally.

2.2 Empirical mode decomposition method: the sifting process

The empirical mode decomposition method is developed from the simple assumption that any signal consists of different simple intrinsic mode oscillations. The essence of the method is to identify the intrinsic oscillatory modes (IMFs) by their characteristic time scale in the signal and then decompose the signal accordingly. The characteristics time scale is defined by the time lapse between the successive extremes.

To extract the IMF from a given data set, a sifting process is implemented as follows. First, identify all the local extrema, and then connect all of the local maxima by a cubic spline line as the upper envelope. Then, repeat the procedure for the local minima to produce the lower envelope. The upper and lower envelopes should cover all the data between them. Their mean is designated $m_1(t)$, and the difference between the data and $m_1(t)$ is $h_1(t)$, i.e.,

$$x(t) - m_1(t) = h_1(t) \tag{1}$$

Ideally, $h_1(t)$ should be an IMF, for the construction of $h_1(t)$ described above should have forced the result to satisfy all the definitions of an IMF by construction. To check if $h_1(t)$ is an IMF, we demand the following conditions: (i) $h_1(t)$ should be free of riding waves, i.e., the first component should not display under-shots or over-shots riding on the data and producing local extremes without zero crossings. (ii) To display symmetry of the upper and lower envelopes with respect to zero. (iii) Obviously the number of zero crossing and extremes should be the same in both functions.

The sifting process has to be repeated as many times as it is required to reduce the extracted signal to an IMF. In the subsequent sifting process steps, $h_1(t)$ is treated as the data, Then

$$h_1(t) - m_{11}(t) = h_{11}(t) \tag{2}$$

where $m_{11}(t)$ is the mean of the upper and lower envelopes $h_1(t)$.

This process can be repeated up to k times; $h_{1k}(t)$ is then given by

$$h_{1(k-1)}(t) - m_{1k}(t) = h_{1k}(t) \tag{3}$$

After each processing step, checking must be done on whether the number of zero crossings equals the number of extrema.

The resulting time series is the first IMF, and then it is designated as $c_1(t) = h_{1k}(t)$. The first IMF component from the data contains the highest oscillation frequencies found in the original data $x(t)$.

This first IMF is subtracted from the original data, and this difference, is called a residue $r_1(t)$ by:

$$x(t) - c_1(t) = r_1(t) \tag{4}$$

The residue $r_1(t)$ is taken as if it was the original data and we apply to it again the sifting process. The process of finding more intrinsic modes $c_i(t)$ continues until the last mode is found. The final residue will be a constant or a monotonic function; in this last case it will be the general trend of the data.

$$x(t) = \sum_{j=1}^{n} c_j(t) + r_n(t) \tag{5}$$

Thus, one achieves a decomposition of the data into n-empirical IMF modes, plus a residue, $r_n(t)$ which can be either the mean trend or a constant.

2.3 The Hilbert-Huang transform (HHT) and its spectrum

Having obtained the IMFs by using EMD method,

one applies the Hilbert transform to each IMF component.

$$H[c_i(t)] = \frac{1}{\pi}\int_{-\infty}^{+\infty}\frac{c_i(\tau)}{t-\tau}\mathrm{d}\tau \tag{6}$$

With this definition $c_i(t)$ and $H[c_i(t)]$ form a complex conjugate pair, which defines an analytic signal $z_i(t)$:

$$z_i(t) = c_i(t) + jH[c_i(t)] \tag{7}$$

Which can be expressed as

$$z_i(t) = a_i(t)\exp(j\omega_i(t)) \tag{8}$$

With amplitude $a_i(t)$ and phase $\theta_i(t)$ defined by the expressions

$$a_i(t) = \sqrt{c_i^2(t) + H^2[c_i(t)]} \tag{9}$$

$$\theta_i(t) = \arctan\left(\frac{H[c_i(t)]}{c_i(t)}\right) \tag{10}$$

Therefore, the instantaneous frequency $\omega_i(t)$ can be given by

$$\omega_i(t) = \frac{\mathrm{d}\theta_i(t)}{\mathrm{d}t} \tag{11}$$

Thus the original data can be expressed in the following form

$$x(t) = \mathrm{Re}\sum_{i=1}^{n} a_i(t)\exp(j\int\omega_i(t)dt) \tag{12}$$

where the residue $r_n(t)$ has been left out. Re $\{.\}$ denotes the real part of a complex quantity.

Eq. (8) enables us to represent the amplitude and the instantaneous frequency in a three-dimensional plot, in which the amplitude is the height in the time-frequency plane. This time-frequency distribution is designated as the Hilbert-Huang spectrum $H(\omega,t)$:

$$H(\omega,t) = \mathrm{Re}\sum_{i=1}^{n} a_i(t)\exp(j\int\omega_i(t)dt) \tag{13}$$

With the Hilbert-Huang spectrum defined, the marginal spectrum, $h(\omega)$, can be defined as

$$h(\omega) = \int_0^T H(\omega,t)\mathrm{d}t \tag{14}$$

where T is the total data length.

The Hilbert spectrum offers a measure of amplitude contribution from each frequency and time, while the marginal spectrum offers a measure of the total amplitude (or energy) contribution from each frequency value. The marginal spectrum represents the cumulated amplitude over the entire data span in a probabilisic sense. As pointed out by Huang et al. [17], the frequency in $h(\omega)$ has a totally different meaning from the Fourier spectral analysis. In the Fourier representation, the existence of energy at a frequency, ω, means a component of a sine or a cosine wave persisting through the time span of the data. Here, the existence of energy at the frequency, ω, means only that, in the whole time span of the data, there is a higher likelihood for such a wave to have appeared locally. In fact, the Hilbert spectrum is a weighted non-normalized joint amplitude-frequency-time distribution. The weight assigned to each time frequency cell is the local amplitude. Consequently, the frequency in the marginal spectrum indicates only the likelihood that an oscillation with such a frequency exists. The exact occurrence time of that oscillation is given in the full Hilbert spectrum.

Therefore, the local marginal spectrum of each IMF component is given as

$$h_i(\omega) = \int_0^T H_i(\omega,t)\mathrm{d}t \tag{15}$$

The local marginal $h_i(\omega)$ spectrum offers a measure of the total amplitude contribution from the frequency ω that we are especially interested in.

3. Proposed marginal spectrum method for fault detection of roller bearing

The procedure of the proposed marginal spectrum method is given as follows:

(1) To calculate the envelope signal $y(t)$ applying Hilbert transform to vibration signal $x(t)$;

$$y(t) = \sqrt{x^2(t) + H^2[x(t)]} \tag{16}$$

(2) To decompose the envelope signal $y(t)$ using EMD and to obtain IMFs;

(3) To select the interested IMF component $c_i(t)$ according to the objective of fault diagnosis;

(4) To calculate the marginal spectrum $h_i(\omega)$ according to Eq. (15);

(5) To analyze the marginal spectrum of selected $c_i(t)$ component and to draw a diagnostic conclusion.

4. Signal simulation of HHT spectrum

In the following section, the results of a simple signal simulation studying the performance of the HHT spectrum are presented to realize a better understanding of this numerical method. For example, Eq. (17) gives one possible mathematical description of the case of a sine wave signal as

$$x(t)=\begin{cases}0 & (0\le t<t_1)\\ \sin(2\pi 30t) & (t_1\le t\le t_2)\\ 0 & (t_2<t\le T)\end{cases} \tag{17}$$

The time domain signal is shown in Fig.1. The sampling time is 0.2s. Let us compare how local the Hilbert-Huang transform can be with the result from FFT, Morlet wavelet and STFT analysis by considering an isolated sine wave given in Fig.1. With Morlet wavelet analysis we get the spectrum in Fig.4, in which the event is well defined on the time axis by the high-frequency components, even though the event is a low-frequency wave. In the result, neither the energy density nor the frequency is well localized; they give a counter-intuitive interpretation of the Morlet wavelet spectrum: to look for definition of a low-frequency event in the high-frequency range. With FFT we get the Fourier spectrum in Fig.2. The Fourier spectrum should give the true frequency distribution, but it fails to give the true frequency of a sine signal. It is obvious that the leakage of the FFT renders the spectrum almost useless. With STFT analysis we get the STFT spectrum in Fig.5. In the result, neither the energy density nor the frequency is well localized. When the same data are treated by the HHT spectral analysis, we have the result in Fig.3, in which the energy is well localized in both frequency and time domains. This simple simulation example illustrates the unique property of the HHT spectrum in elimination of the spurious harmonic components to represent the non-stationary data.

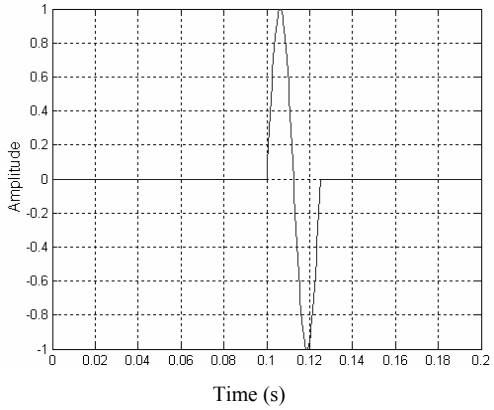

Fig. 1. Time domain signal of a sine wave signal.

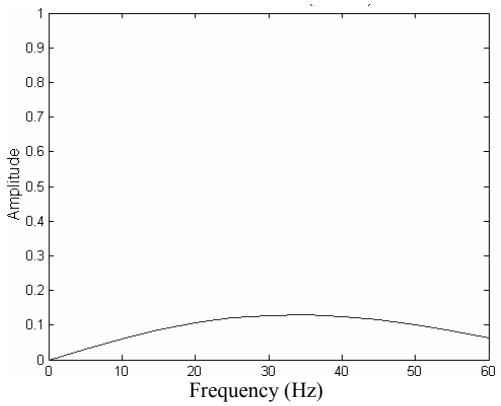

Fig. 2. FFT of a sine wave signal.

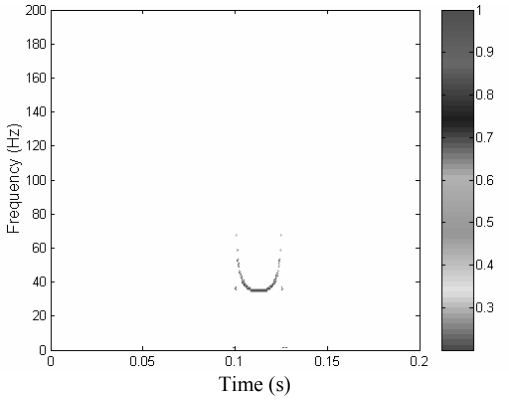

Fig. 3. HHT spectrum of a sine wave signal.

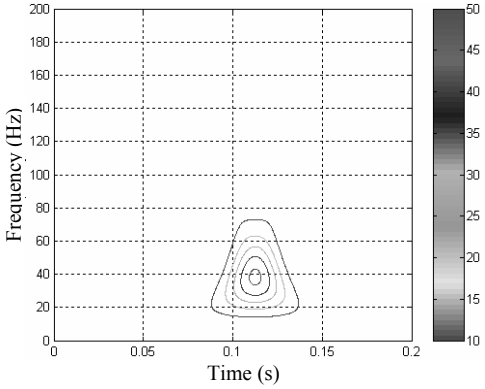

Fig. 4. Morlet wavelet of a sine wave signal.

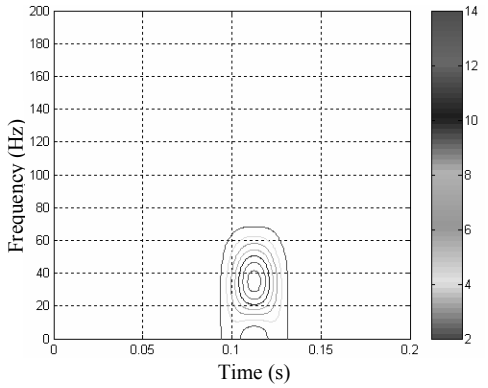

Fig. 5. STFT spectrum of a sine wave signal.

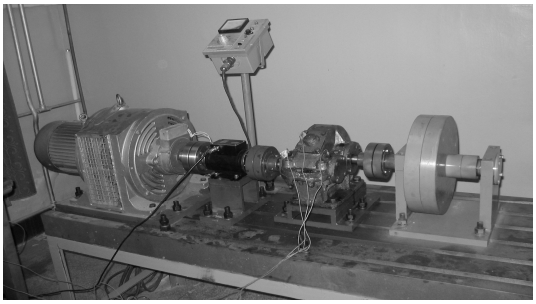

Fig. 6. Experimental set-up.

5. Experimental set-up

The test apparatus used in this study is shown in Fig. 6. The experimental set-up consists of a single-stage gearbox, driven by a 4.5 kW AC governor motor. The driving gear has 28 teeth and the driven gear has 36 teeth. Therefore, the transmission ratio is 36/28, which means that a decrease in rotation speed is achieved. The module of the gear is 2.5mm. The input speed of the spindle is 1500r/min, that is, the rotating frequency f_r of the input shaft is 25 Hz. The monitoring and diagnostic system is composed of three accelerometers, amplifiers, a speed and torque transducer, B&K 3560 spectrum analyzer and a computer. The sampling frequency is 16384 Hz and the sampling point is 2048. After sampling, the measured vibration signals were loaded into MATLAB from data-files.

6. Roller bearing fault detection and diagnosis based on marginal spectrum

Roller bearings are installed in many kinds of machinery. Many problems of those machines may be caused by defects of the roller bearing. Generally, local defects may occur on inner race, outer race or rollers of bearing. A local fault may produce periodic impacts, the size and the repetition period which are determined by the shaft rotation speed, the type of fault and the geometry of the bearing. The successive impacts produce a series of impulse responses, which may be amplitude modulated because of the passage of fault through the load zone. The spectrum of such a signal would consist of a harmonics series of frequency components spaced at the component fault frequency with the highest amplitude around the resonance frequency. These frequency components are flanked by sidebands if there is an amplitude modulation due to the load zone. According to the period of the impulse, we can judge the location of the defect using characteristic frequency formulae. Because an inner race defect has more transfer segments when transmitting the impulse to the outer surface of the case, usually the impulse components are rather weak in the vibration signal.

The tested bearing was used to study only one kind of surface failure: the bearing was damaged on the inner race or outer race. The roller bearing tested has a groove on the inner race or outer race. Localized defect was seeded on the inner race or outer race by an electric-discharge machine to keep their size and depth under control. The size of the artificial defect was 1mm in depth and the width of the groove was 1.5mm. The type of the roller bearing is 208. There are 10 rollers in a bearing and the contact angle $\alpha = 0°$, roller diameter d= 55/3 mm, bearing pitch diameter D=97.5mm. Then the characteristic frequency of the inner or outer race defect can be calculated by Eq. (18) or Eq. (19).

$$f_{inner} = \frac{z}{2}\left(1 + \frac{d}{D}\cos\alpha\right) f_r \tag{18}$$

$$f_{outer} = \frac{z}{2}\left(1 - \frac{d}{D}\cos\alpha\right) f_r \tag{19}$$

Therefore, according to Eq. (18) and Eq. (19), the characteristic frequency of the inner race defect is calculated to be at 148.5Hz, and the characteristic frequency of the outer race defect is calculated to be at 101.5Hz .

6.1 Application of marginal spectrum to fault detection and diagnosis of inner race

The original vibration signal of inner race defect is

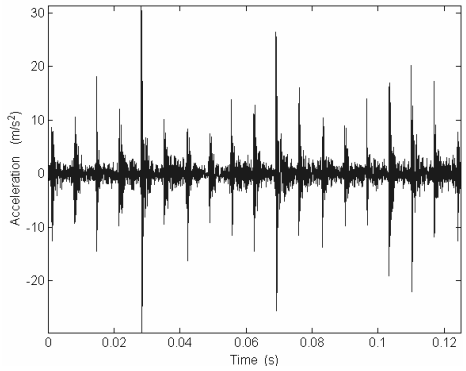

Fig. 7. Time-domain vibration signal with inner fault.

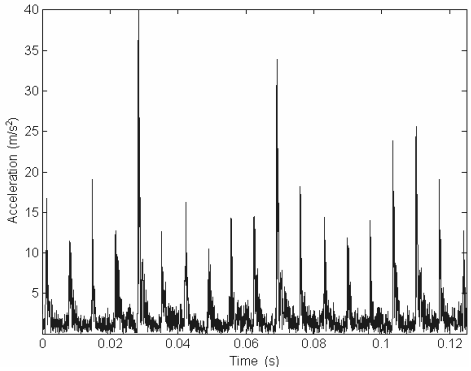

Fig. 8. Envelope signal of the vibration signal with inner fault.

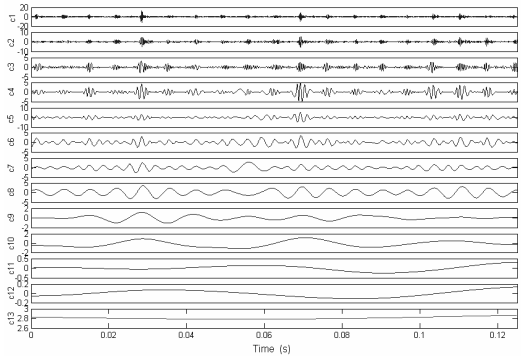

Fig. 9. IMFs of the envelope signal shown in Fig. 8.

displayed in Fig. 7. It is clear that there are periodic impacts in the vibration signal. There are significant fluctuations in the peak amplitude of the signal, and there are also considerable variations of frequency content. Fig.8 shows the envelope signal of the vibration signal, which is computed according to Eq. (16).

To the data of Fig.8, the EMD algorithm is applied. Fig. 9 displays the empirical mode decomposition in thirteen IMFs of the envelope signal in Fig. 8. The

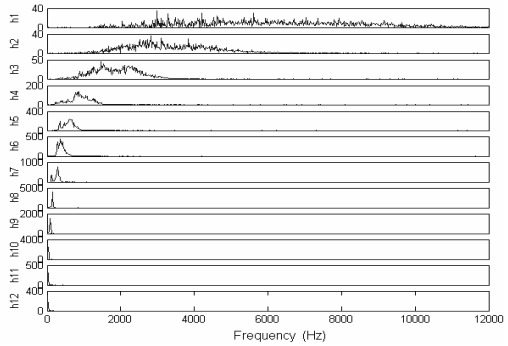

Fig. 10. Marginal spectrum of IMFs.

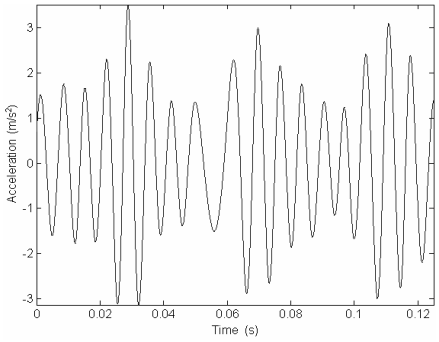

Fig. 11. IMF component c_8.

decomposition identifies thirteen modes: c_1 - c_{12}, which represent the different frequency components excited by the inner race defects, and c_{13} is the residue, respectively. Mode c_1 contains the highest signal frequencies, mode c_2 the next higher frequency band and so on.

From Fig. 9, it can be easily proven that the EMD decomposes the vibration signal very effectively on an adaptive method. The Hilbert-Huang transform can be applied to each IMF $c_i(t)$, resulting in a marginal spectrum $h_i(\omega)$ according to Eq. (15). The marginal spectrum $h_i(\omega)$ is shown in Fig.10. From Fig.10, we can know that the mode c_1 with marginal spectrum is centered from 2000 Hz to 10000 Hz, mode c_2 with marginal spectrum centered from 2000 Hz to 5000 Hz, mode c_3 with marginal spectrum centered from 1000 Hz to 3000 Hz and mode c_4 with marginal spectrum centered at 1000 Hz. Therefore, it is can be concluded that modes c_1 - c_2 are the high frequency vibration excited by inner race faults of the roller bearing. The mode c_8 with marginal spectrum is centered at 148.5Hz, which can be obviously associated with the characteristic frequency of the inner race defect. Modes c_9, c_{10} and c_{11} are

associated with the high harmonic of the rotational frequency of the input shaft. The mode c_{12} is associated with the rotational frequency of the input shaft itself (25Hz). Moreover, the amplitude of the marginal spectrum h_8 is larger than that of the others. So it can be concluded that the fault occurred in the inner race of the roller bearing. Therefore, it seems that mode c_8 is related to inner race defect of the roller bearing. The zoomed figures of c_8 and h_8 are displayed in Fig. 11 and Fig. 12, respectively.

6.2 Application of marginal spectrum to fault detection and diagnosis of outer race

The original vibration signal of an outer race defect is displayed in Fig. 13. Fig. 14 shows the envelope signal of the vibration signal. Fig. 15 displays the empirical mode decomposition in eight IMFs of the envelope signal in Fig. 14. The decomposition identifies eight modes: c_1 - c_7 represent the frequency components excited by the outer race defects, c_8 is the residue, respectively. Mode c_1 contains the highest signal frequencies, mode c_2 the next higher frequency band and so on.

The Hilbert-Huang transform can be applied to each IMF $c_i(t)$, resulting in marginal spectrum $h_i(\omega)$ according to Eq. (15). This is shown in Fig.16. From Fig.16, we can know that the mode c_1 with marginal spectrum is centered from 400 Hz to 1500 Hz, mode c_2 with marginal spectrum centered from 200 Hz to 800 Hz and mode c_3 with marginal spectrum centered at 250 Hz. Therefore, it can be concluded that modes c_1 - c_2 are the high frequency vibration excited by outer faults of the bearing. The mode c_4 with marginal spectrum is centered at 101.5Hz, which can be obviously associated with the characteristic frequency of the outer race defect. Modes c_5 and c_6 are associated with the high harmonic of the rotational frequency of the input shaft. The mode c_7 is associated with the rotational frequency of the input shaft itself (25Hz). Moreover, the amplitude of the marginal spectrum h_4 is larger than that of the others. So it can be concluded that the fault

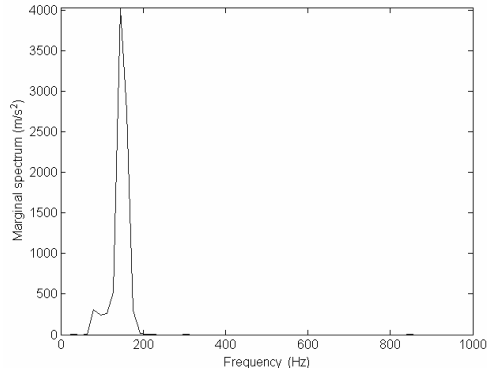

Fig. 12. Marginal spectrum of IMF c_8.

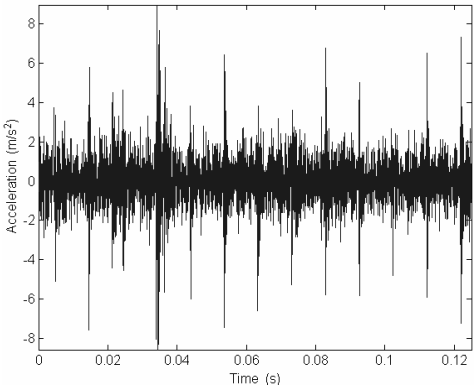

Fig. 13. Time-domain vibration signal with outer fault.

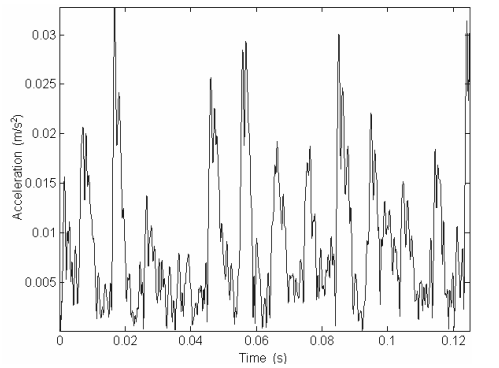

Fig. 14. Envelope signal of the vibration signal with outer fault.

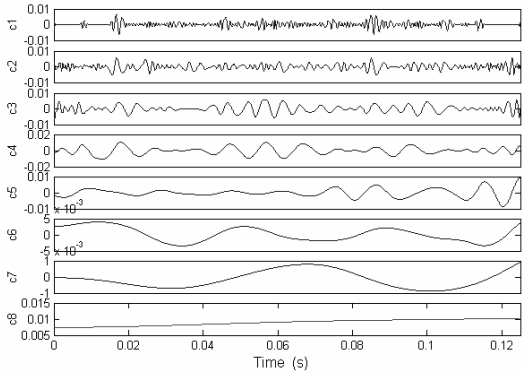

Fig. 15. IMFs of the envelope signal shown in Fig. 14.

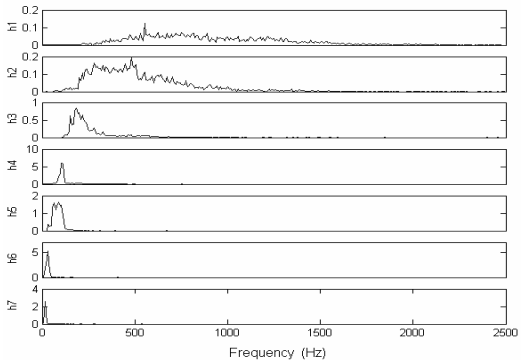

Fig. 16. Marginal spectrum of IMFs.

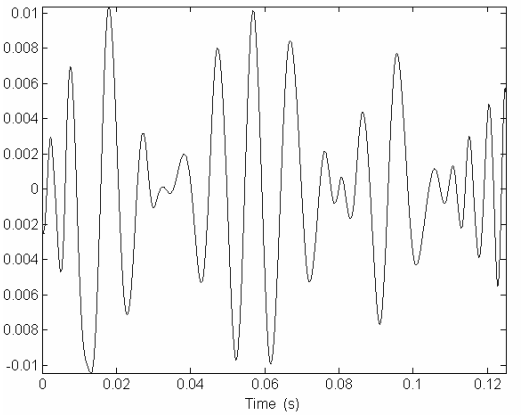

Fig. 17. IMF component c_4.

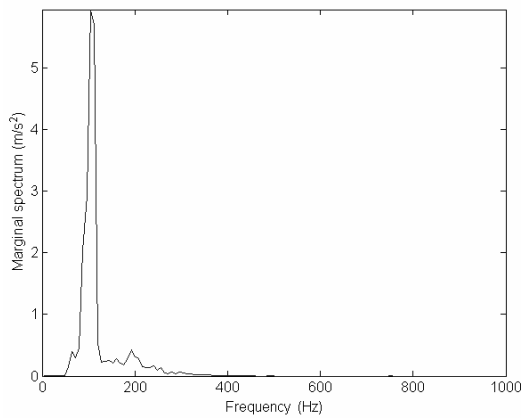

Fig. 18. Marginal spectrum of IMF c_4.

occurred in the outer race of the roller bearing. There fore, it seems that mode c_4 is related to the outer race defect of the roller bearing. The zoomed figures of c_4 and h_4 are displayed in Fig. 17 and Fig. 18, respectively.

7. Conclusions

A method for fault diagnosis of roller bearings was presented based on a newly developed signal processing technique named as Hilbert-Huang transform and its marginal spectrum. Using EMD method, the original vibration signals of roller bearing faults can be decomposed into intrinsic modes. Therefore, we can recognize the vibration modes that coexist in the system, and have a better understanding of the nature of the fault information contained in the vibration signal. According to the marginal spectrum, the characteristic frequency of the roller bearing faults can be easily recognized. Practical vibration signals monitored from roller bearings with inner or outer race fault are analyzed by the presented method. The experimental result has shown that marginal spectrum can be used as a diagnostic feature for roller bearing faults.

Acknowledgment

The authors are grateful to the National Natural Science Foundation of China (No.50775219 and No.50375157), Zhejiang Provincial Natural Science Foundation (No.Y1080040). The authors are also grateful for the editors and reviewers who made constructive comments.

References

[1] L. Cohen, *Time-frequency analysis*, Prentice-Hall, Englewood Cliffs, NJ, 1995.

[2] J. Lin and L. Qu, Feature extraction based on Morlet wavelet and its application for mechanical fault diagnosis, *Journal of Sound and Vibration*, 234(1) (2000) 135-148.

[3] W. J. Staszewski, Wavelet based compression and feature selection for vibration analysis, *Journal of Sound and Vibration*, 211(5)(2000) 736-760.

[4] C. James Li and Jun Ma, Wavelet decomposition of vibration for detection of bearing-localized defects, *NDT&E International*, 30(3)(1997) 143-149.

[5] S. Prabhakar, A. R. Mohanty and A. S. Sekhar, Application of discrete wavelet transform for detection of ball bearing race fault, *Tribology International*, 3(12)(2002) 793-800.

[6] W. J. Wang and P. D. Mcfadden, Application of orthogonal wavelet to early gear damage detection, *Mechanical Systems and Signal Processing,* 9(5)

(1995) 497-507.

[7] W. J. Staszewski, K. Worden and G. R. Tomlinson, The-frequency analysis in gearbox fault detection using the Wigner-Ville distribution and pattern recognition, *Mechanical Systems and Signal Processing*, 11(5)(1997) 673-692.

[8] L. Galleani and L. Cohen, The Wigner distribution for classical system, *Physics Letters A*, 302(4)(2002) 149-155.

[9] G. Matz and F. Hlawatsch, Wigner distribution (nearly) everywhere: time-frequency analysis of signals, systems, random process, signal spaces, and frames, *Signal Processing,* 83(7)(2003) 1355-1378.

[10] B. Boashash, *Time-frequency signal analysis and processing*, Prentice-Hall, Englewood Cliffs, NJ, 2003.

[11] F. Hlawatsch and W. Kozek, The Wigner distribution of a linear signal space, *IEEE transaction on signal process,* 41(3)(1993) 1248-1258.

[12] T. J. Wahl and J. S. Bolton, The application of the Wigner distribution to the identification of structure-borne noise components, *Journal of Sound and Vibration,* 163(1)(1993) 101-122.

[13] H. O. Bartelt, K. H. Brenner and A. W. Lohmann, The Wigner distribution function and its optical production, *Optics Communications,* 32(1980) 32-38.

[14] Q. Meng and L. Qu, Rotating machinery fault diagnosis using Wigner distribution, *Mechanical Systems and Signal Processing,* 5(3)(1991) 155-166.

[15] J. Leuridan and H. V. D. Auweraer, The analysis of non-stationary dynamics signals, *Sound and Vibration,* 11(1994) 14-26.

[16] Y. S. Shin and J. J. Jeon, Pseudo Wigner-Ville time-frequency distribution and its application to machinery condition monitoring, *Shock and Vibration,* 1(1993) 65-76.

[17] N. E. Huang, Z. Shen and S. R. Long et al, The empirical mode decomposition and the Hilbert spectrum for nonlinear and non-stationary time series analysis, *Proceedings of the Royal Society London, Series A,* 454(1998) 903-995.

[18] W. Huang, Z. Shen, N. E. Huang and Y. C. Fung, Nonlinear Indicial Response of Complex Nonstationary Oscillations as Pulmonary Hypertension Responding to Step Hypoxia, *Proc of the National Academy of Sciences*, *USA,* 96(1999) 1834-1839.

[19] W. Huang, Z. Shen, N. E. Huang and Y. C. Fung, Engineering Analysis of Biological Variables: An Example of Blood Pressure over One Day, *Proc of the National Academy of Sciences*, *USA,* 95(1998) 4816-4821.

[20] W. Huang, Z. Shen, N. E.Huang and Y. C. Fung, Engineering Analysis of Intrinsic Mode and Indicial Response in Biology: the Transient Response of Pulmonary Blood Pressure to Step Hypoxia and Step Recovery, *Proc of the National Academy of Science*,*USA,*95(1998) 12766-12771.

[21] N. E. Huang, Z. Shen and S. R. Long, A new view of nonlinear water waves: The Hilbert spectrum, *Annual Review of Fluid Mechanics,* 31(1999) 417-457.

[22] L. Wang, C. Koblinsky, S. Howden and N. E. Huang, Interannual Variability in the South China Sea from Expendable Bathythermograph Data, *Journal of Geophysical Research,*104(10)(1999) 23509-23523.

[23] M. L. Wu, S. Schubert, N. E. Huang, The Development of the South Asian Summer Monsoon and the Intraseasonal Oscillation, *Journal of Climate,* 12(7) (1999) 2054-2075.

[24] M. Datig and T. Schlurmann, Performance and limitations of the Hilbert-Huang transformation (HHT) with an application to irregular water waves, *Ocean Engineering,* 31(14-15)(2004) 1783-1834.

[25] J. Nunes, Y. Bouaoune, E. Delechelle, O. Niang and P. Bunel, Image analysis by bidimensional empirical mode decomposition, *Image and Vision Computing*, 21(12)(2003) 1019-1026.

[26] S. Quek, P. Tua and Q. Wang, Detecting anomalies in beams and plate based on the Hilbert-Huang transform of real signals, *Smart Materials and Structures*,12(3)(2003) 447-460.

[27] S. J. Loutridis, Damage detection in gear system using empirical mode decomposition, *Engineering Structure,* 26(12)(2004) 1833-1841.

[28] Hui Li, Yuping Zhang and Haiqi Zheng, Wear Detection in Gear System Using Hilbert-Huang Transform. *Journal of Mechanical Science and Technology (KSME Int.J.)*, 20(11)(2006)1781-1789.

[29] Hui Li, Haiqi Zheng, Liwei Tang, Wigner-Ville Distribution Based on EMD for Faults Diagnosis of Bearing, *Lecture Notes in Computer Science*, 4223 (2006)803-812.

[30] M. Montesinos, J. Munoz-Cobo, C. Perez, Hilbert-Huang analysis of BWR detector signals: application to DR calculation and to corrupted signal analysis, *Annals of Nuclear Energy,* 30(6)(2003) 715-727.

Hui Li received his B.S. degree in mechanical engineering from the Hebei Polytechnic University, Hebei, China, in 1991. He received his M.S. degree in mechanical engineering from the Harbin University of Science and Technology, Hei-longjiang, China, in 1994. He re-ceived his PhD degree from the School of Mechanical Engineering of Tianjin University, Tianjin, China, in 2003. He is currently a professor in mechanical engineering at Shijiazhuang Institute of Railway Technology, China. His research and teaching interests include hybrid driven mechanism, kinematics and dynamics of machinery, mechatronics, CAD/CAPP, signal processing for machine health monitoring, diagnosis and prognosis.